

Application of synchrotron radiation X-ray fluorescence imaging combined with histochemical staining to the renal section of mercury-treated rats

S. Homma-Takeda,^{a*} Y. Kumagai,^a M. Shinyashiki^b and N. Shimojo^a

^aDepartment of Environmental Medicine, Institute of Community Medicine, University of Tsukuba, Tsukuba, Ibaraki 305, Japan, and ^bGraduate School of Environmental Sciences, University of Tsukuba, Tsukuba, Ibaraki 305, Japan. E-mail: shino-bv@md.tsukuba.ac.jp

(Received 16 June 1997; accepted 8 September 1997)

A combination method consisting of synchrotron radiation X-ray fluorescence imaging and histochemical staining was employed to examine the detailed distribution of metal elements and morphological changes in the kidney section of rats exposed simultaneously to mercurial. A single injection of mercuric chloride (5 mg kg^{-1}) to rats resulted in significant urinary leakages of the biological markers for acute mercury intoxication. Under this condition (i) a striking damage of brush border, cell loss and a dominant accumulation of mercury in the proximal tubules, (ii) a good correlation between the tubular damage caused by mercury and localization of the toxic metal, and (iii) an obvious distribution difference between zinc and sulfur following mercury exposure, were successfully shown by the present procedure with a $20 \text{ }\mu\text{m}$ -thick specimen.

Keywords: X-ray fluorescence analysis; copper; mercury; zinc; zinc; rat; kidneys.

1. Introduction

Application of synchrotron-radiation-excited X-ray fluorescence analysis to biomedical samples has provided important information about the alternation of trace elements in a variety of organs (Gordon *et al.*, 1990; Kwiatek *et al.*, 1990; Yao, Zhang, Wu, Zhu & Zheng, 1993; Homma *et al.*, 1993; Homma, Nakai, Misawa & Shimojo, 1995; Shimojo *et al.*, 1997) because the tunability of the energy spectrum is useful for multi-elemental analysis, and the brightness and collimation of synchrotron radiation are suitable for microbeam analysis. Moreover, the minimal radiation damage of synchrotron radiation X-ray fluorescence (SR-XRF) to specimens compared with other analyses using ion or electron probes should allow researchers to investigate the distribution of elements, followed by changes in cells or tissues caused by drug and disease with the same specimen. However, there are few studies on the simultaneous determination of SR-XRF imaging to detect elements and histopathological alternation to distinguish the type of cells.

Mercury is a nephrotoxic metal and is thought to cause more serious damage to the proximal tubules than to the distal tubules or glomeruli (Fowler, 1992; Siegel & Bulger, 1975). In our previous examination we demonstrated high correlations between Hg and essential trace elements, such as copper, selenium and zinc, which distributed in the tissues of animals exposed to mercuric

compounds (Shimojo, Homma, Nakai & Iida, 1991; Homma & Shimojo, 1991). In this study we have extended the method to a combination analysis which allows the determination of morphological change by histochemical staining and Hg distribution by SR-XRF imaging using an X-ray microprobe after the metal exposure. The elemental maps of Cu, S and Zn corresponding to the histopathological data are also shown.

2. Experimental

2.1. Specimen preparation

HgCl_2 was dissolved in saline and administered to male Wistar rats (eight weeks old, five rats per group, housed in individual metabolic cages) by subcutaneous injection at a dose of 5 mg kg^{-1} . The rats were killed under ether anesthesia for collection of kidney and blood samples 24 h after the administration. Renal samples from one kidney of each rat were fixed in 10% buffered formalin, embedded in acrylic resin, and then cut into $20 \text{ }\mu\text{m}$ -thick cross sections by a microtome (Jung polycut E, Leica Instruments GmbH, Germany) with a tungsten knife (type D, Leica Instruments GmbH, Germany) for the specimens for SR-XRF analysis. Urine, collected for 24 h after the administration, and blood were used for the evaluation of nephrotoxicity. Alkaline phosphatase (Bessey, Lowry & Brock, 1946) and *N*-acetyl- β -glucosaminidase (Noto *et al.*, 1983) activities in urine and serum blood urea nitrogen (Searcy, Foreman, Kezt & Readon, 1967) were measured using commercial kits from Wako Pure Chemical Industries Ltd (Osaka, Japan). The total protein content in the urine was determined by the method of Bradford (1976) with bovine serum albumin as a standard.

2.2. Combination analysis of SR-XRF with PAS staining

XRF measurements for Hg, Zn, Cu and S were made at the Photon Factory, National Laboratory for High Energy Physics, Tsukuba, Japan, utilizing an energy-dispersive SR-XRF system with monochromatic X-ray microbeams obtained by a multilayer monochromator and K-B-type focusing optics (Iida & Noma, 1993). Two-dimensional analysis was carried out by placing a sample on an *XY* stage according to the method of Iida & Noma (1993) with slight modification: the X-ray energy was 14.38 keV , the beam size $5 \times 6 \text{ }\mu\text{m}^2$, the step size $5 \text{ }\mu\text{m step}^{-1}$ and the counting time 10 s point^{-1} . The X-ray intensity data of the Hg $L\alpha$, Zn $K\alpha$, Cu $K\alpha$ and S $K\alpha$ fluorescence lines (Fig. 1) of each point were processed with a personal computer, and the results were shown as a tone from black to white classified into 14 degrees from

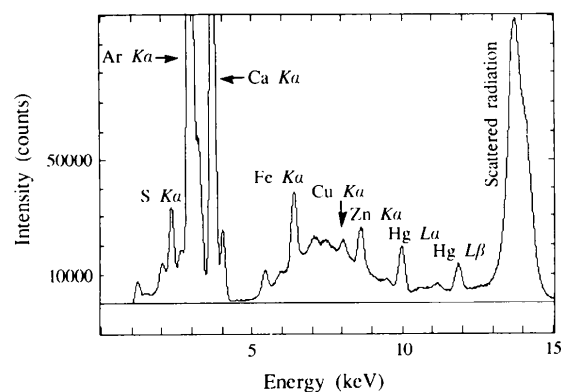


Figure 1
X-ray fluorescence spectrum obtained from the Hg-treated rat kidney. The collection time was 10 000 s.

maximum to minimum that are linearly proportional to the 14 levels of the element concentrations. Since the elemental imaging data are semiquantitative, the other kidney of each rat was wet-digested and then Cu and Zn levels were measured by inductively coupled plasma atomic emission spectrometry (ICP-AES) as described earlier (Homma *et al.*, 1993), and Hg concentrations were measured by flameless atomic absorption spectrometry (FAAS) (Jacobs, Yamaguchi, Goldwater & Gilbert, 1960). For histopathological determination the same sample was stained by

the method of periodic acid Schiff (PAS) reaction (Thompson, 1966), followed by counter-staining (nuclei) with Carrazzi's hematoxylin.

3. Results and discussion

When HgCl_2 (5 mg Hg kg^{-1}) was subcutaneously injected into the rats, excretions of biological markers of the renal tubular damage caused by the metal, such as alkaline phosphatase, *N*-acetyl- β -glucosaminidase, and total protein, were extremely high in the urine (Fig. 2). A significant increase in blood urea nitrogen level, which is an indicator of glomerular failure, was also observed. Under the circumstances, PAS staining confirmed that there were damages of brush border and cell loss in the proximal tubules in the renal specimen of rat exposed to mercurial as shown in Fig. 3(a). Two-dimensional distributions of Hg, Zn and S in the same section were clearly obtained whereas that of Cu was obscure (Figs. 3c–3f).

Corresponding to SR-XRF imaging with PAS staining, Hg accumulated more in renal tubules (T1–T13) than in glomeruli (G) (Fig. 3c). Among the renal tubules, Hg was higher in the damaged proximal tubules (T5, T7, T9, T10, T11 and T13) compared with the fine undamaged proximal tubules (T2, T3, T6 and T12), the distal tubules (T8), or the collecting tubules (T4). Upon further analysis, Hg was found to be higher in the periphery of the proximal tubules for the damaged tubules (T5, T7, T9, T10, T11 and T13), while Hg was higher in the central area, that is, brush border of the undamaged tubules (T2, T3, T6 and T12). The Zn

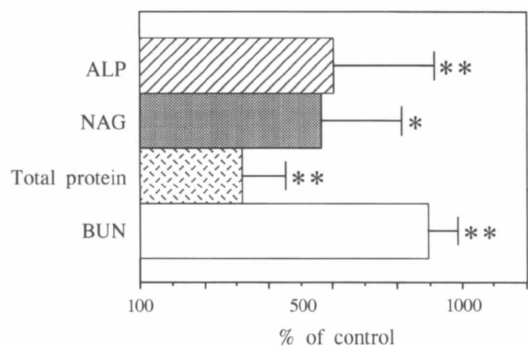


Figure 2

Effects of mercury treatment on the renal functions. ALP: alkaline phosphatase; NAG: *N*-acetyl- β -glucosaminidase; BUN: blood urea nitrogen. For control, untreated rats were used. Data indicate the mean \pm standard deviation of five rats. * significant difference between HgCl_2 and control rats ($P < 0.05$); ** $P < 0.01$.

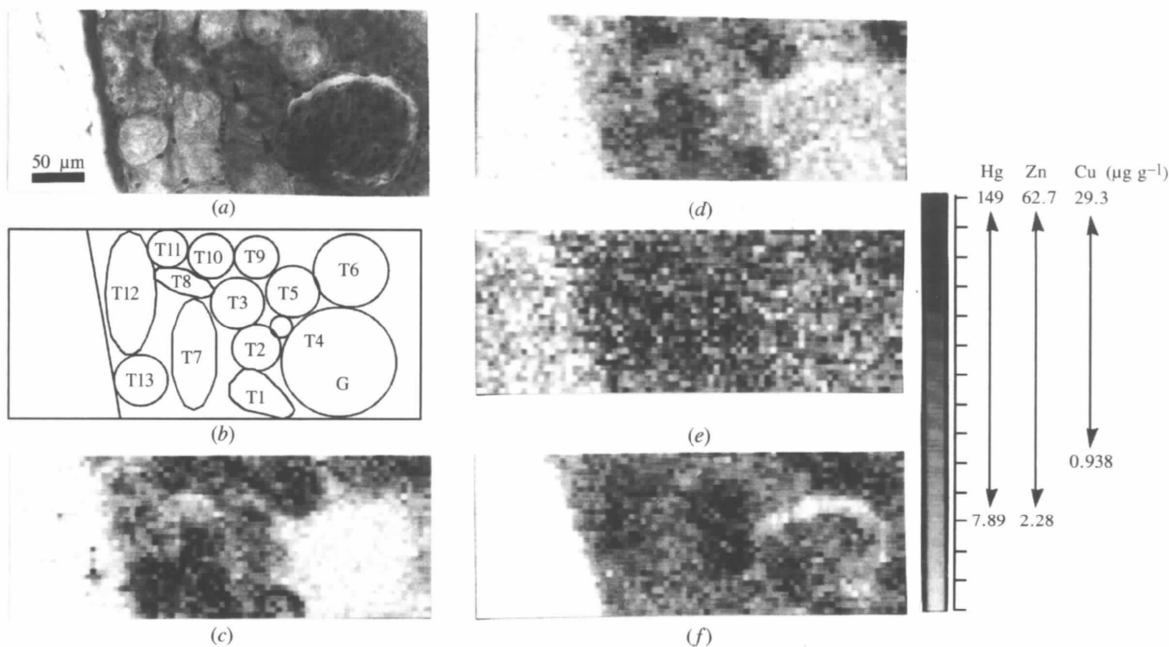


Figure 3

PAS staining (a) and SR-XRF imaging (c)–(f) of the kidney of the rat administered Hg. (b) an illustration of (a); (c) the distribution of Hg, (d) Zn, (e) Cu, (f) S. The sample scanning condition was 75×29 steps with $5 \mu\text{m step}^{-1}$. PAS staining is an appropriate method for distinguishing several types of renal cells; the brush borders (arrows), which are a characteristic structure of the proximal tubules, are stained by the PAS reaction. Many nuclei and thin tubules distinguish the distal tubules (T8) from the proximal tubules. Elemental concentration ranges of XRF imaging were calculated using the Hg (determined by FAAS), Cu and Zn (by ICP-AES) concentrations in the specimen. The pixels of the lower value of elemental concentration range are background pixels. [The Hg concentration in the renal specimen of Fig. 3 determined by FAAS was $45.2 \mu\text{g g}^{-1}$, and its Cu and Zn levels by ICP-AES were 6.77 and $19.4 \mu\text{g g}^{-1}$, respectively. Under the experimental conditions the estimated minimum detection limits (MDLs) of these metals for the XRF measurement were 7.01 (Hg), 4.42 (Cu) and $4.33 \mu\text{g g}^{-1}$ (Zn) according to the following equation (Iida & Gohshi, 1991). $\text{MDL} = 3C_i N_b^{1/2} / (N_p - N_b)$, where N_b is the mean of the relative X-ray intensity at the background, N_p is mean of the relative X-ray intensity at the tissue, and C_i is the element concentration estimated by FAAS or ICP-AES (see above). For this reason, $20 \mu\text{m}$ -thick specimens rather than $10 \mu\text{m}$ -thick sections were used in this study to obtain clear imaging.]

distribution exhibited a similar tendency (proximal tubules > distal tubules > glomeruli with damaged tubules > undamaged tubules). In contrast, sulfur content was higher in the undamaged tubules than the damaged ones. The glomerulus had a lower sulfur content compared with the renal tubules.

In the present study we improved the spatial resolution of SR-XRF imaging, *i.e.* from $500 \times 500 \mu\text{m}^2$ in our previous study to $5 \times 5 \mu\text{m}^2$. In other words the elemental imaging of the present method is able to distinguish the various types of renal cells, whereas only the renal medulla and cortex are distinguishable in the previous study (Homma & Shimojo, 1991). In our preliminary study high correlations ($r = 0.656$ – 0.920) were shown between the Hg and Zn distribution in the kidneys of rats exposed to organic mercury compounds (Homma & Shimojo, 1991). A similar relationship was also supported by the present method ($r = 0.582$). This slight decrease in correlation of these elements may be due to differences in the grade of renal tubular damage. As shown in Fig. 3, however, the distribution of Hg in the specimen was not necessarily consistent with that of S ($r = 0.169$), in spite of the fact that Hg has a high affinity for thiol function (Clarkson, 1972). A reasonable explanation for this discrepancy seems to be attributable to a leakage of intracellular proteins occurring by severe cellular damage during mercury exposure because cysteine is a dominant amino acid in many of the protein components.

After SR-XRF analysis, a breach and a scorching of the specimen were not observed while the analyzed area seemed to be stained slightly stronger than the non-examined area. Nevertheless, the fixed samples used in this study, which are no longer in their native state of trace elements, provide us with useful information when trace elements bound to proteins, not the free-ion form, are investigated, although, for imaging samples for SR-XRF, tissue sections prepared under cryogenic conditions would be required. Moreover, the specimen of the hydrophilic acrylic lesion is easy to deal with when specimens are set on the XY stage and suitable for not only histochemical (*e.g.* hematoxylin, eosin and methylgreen) staining but also immunohistochemical (*e.g.* ABC method) staining (data not shown). Therefore, the procedure described in this study would be one of the techniques for the biomedical application of SR-XRF microbeam analysis.

This study was performed under the approval of the Photon Factory Advisory Council (proposal Nos. 93 G095, 94 G095). We are grateful to Dr A. Iida, Photon Factory, National Laboratory for

High Energy Physics, for his kind advice during the experiments at the Photon Factory. Thanks are also due to Dr I. Nakai, Department of Applied Chemistry, Science University of Tokyo, for his help during the experiments. The authors also thank Dr E. Suzuki and Mr T. Mori, Department of Pathology, Tsukuba University Hospital, for their constructive comments during histochemical staining. This work was supported by the Scientific Research Grant-in-Aid No. 08770248 from the Ministry of Education, Science and Culture, Japan.

References

- Bessey, O. A., Lowry, O. H. & Brock, M. J. (1946). *J. Biol. Chem.* **164**, 321–329.
- Bradford, M. M. (1976). *Anal. Biochem.* **72**, 248–254.
- Clarkson, T. W. (1972). *Annu. Rev. Pharmacol.* **12**, 375–406.
- Fowler, B. A. (1992). *Environ. Health Perspect.* **100**, 57–63.
- Gordon, B. M., Jones, K. W., Hanson, A. L., Pounds, J. G., Rivers, M. L., Spanne, P. & Sutton, S. R. (1990). *Biol. Trace Elem. Res.* **26/27**, 133–141.
- Homma, S., Nakai, I., Misawa, S. & Shimojo, N. (1995). *Nucl. Instrum. Methods Phys. Res. B.* **103**, 229–232.
- Homma, S., Sasaki, A., Nakai, I., Sagai, M., Koiso, K. & Shimojo, N. (1993). *J. Trace Elem. Exp. Med.* **6**, 163–170.
- Homma, S. & Shimojo, N. (1991). *Biomed. Res. Trace Elem.* **2**, 51–56. (In Japanese.)
- Iida, A. & Gohshi, Y. (1991). *Handbook on Synchrotron Radiation*, Vol. 4, edited by S. Ebashi, M. Koch & E. Rubenstein, pp. 307–348. Amsterdam: Elsevier Science.
- Iida, A. & Noma, T. (1993). *Nucl. Instrum. Methods Phys. Res. B.* **82**, 129–138.
- Jacobs, M. B., Yamaguchi, S., Goldwater, L. J. & Gilbert, H. (1960). *Am. Ind. Hyg. Assoc. J.* **21**, 475–480.
- Kwiatek, W. M., Long, G. J., Pounds, J. G., Reuhl, K. R., Hanson, A. L. & Jones, K. W. (1990). *Nucl. Instrum. Methods Phys. Res. B.* **49**, 561–565.
- Noto, A., Ogawa, Y., Mori, S., Yoshida, M., Kitakaze, T., Hori, T., Nakamura, M. & Miyake, T. (1983). *Clin. Chem.* **29**, 1713–1716.
- Searcy, R. L., Foreman, J. A., Ketz, A. & Reardon, J. (1967). *Am. J. Clin. Pathol.* **37**, 667–681.
- Shimojo, N., Homma, S., Nakai, I. & Iida, A. (1991). *Anal. Lett.* **24**, 1767–1777.
- Shimojo, N., Homma-Takeda, S., Ohuchi, K., Shinyashiki, M., Sun, G. F. & Kumagai, Y. (1997). *Life Sci.* **60**, 2129–2137.
- Siegel, F. L. & Bulger, R. E. (1975). *Virchows. Arch. B.* **18**, 243–262.
- Thompson, S. W. (1966). *Selected Histochemical and Histopathological Methods*, edited by S. W. Thompson & Charles C. Thomas, pp. 480–496. Illinois: Springfield.
- Yao, H., Zhang, J., Wu, X., Zhu, J. & Zheng, X. (1993). *Nucl. Instrum. Methods Phys. Res. B.* **75**, 563–566.